PAPER DETAILS

TITLE: Characterization of Micro-seismic Activity in Northern Cyprus Using Complexity and Corner Frequency Methods

AUTHORS: Evrim Yavuz

PAGES: 884-898

ORIGINAL PDF URL: https://dergipark.org.tr/tr/download/article-file/3370170

Sakarya University Journal of Science

ISSN : 2147-835X
Publisher : Sakarya University

Vol. 28, No. 4, 884-898, 2024
DOI: https://doi.org/10.16984/saufenbilder.1351756

Research Article

Characterization of Micro-seismic Activity in Northern Cyprus Using Complexity and Corner Frequency Methods

Evrim Yavuz

İstanbul Metropolitan Municipality, Department of Earthquake Risk Management and Urban Improvement, Directorate of Earthquake and Ground Research, İstanbul, Türkiye, evrim.yavuz@ibb.gov.tr

ARTICLE INFO

Keywords:
Discrimination functions
Complexity
Cyprus
Corner frequency
Seismic event

Article History:
Received: 29.08.2023
Accepted: 30.07.2024
Online Available: 06.08.2024

ABSTRACT

Cyprus is an island country located in the eastern Mediterranean, to the south of Türkiye and the western of Syria and Lebanon, and is a popular tourist destination. Due to being surrounded by seas on all four sides, meticulous planning of rescue, assistance, and evacuation plans is necessary in the face of disasters such as earthquakes and tsunamis. Tectonically, the southern part of the island is controlled by the Cyprus Arc, while the northern part is dominated by the Kyrenia Range. The demand for raw materials for construction and industry is met through controlled quarry blasting operations carried out by open-pit quarry companies in the districts of Kyrenia and Nicosia. As a result, both natural and artificial seismic events occur in the region, and these quakes are documented in seismic catalogs by seismology centers. However, due to the low energy content of micro-seismic events and the inadequacy of seismic stations on the island, the source types of these seismic events can be misidentified in the catalogs. In this context, the study focuses on 122 seismic events with magnitudes between $0.9 \leq Ml \leq 2.7$ that occurred in Northern Cyprus during the January 2018 - December 2021 period (4 years). The seismic events recorded by the station LFK, operated by Boğaziçi University Kandilli Observatory and Earthquake Research Institute Regional Earthquake-Tsunami Monitoring Center (KOERI-RETMC), were classified using Linear and Quadratic Discriminant Functions based on complexity and corner frequency methods. According to the results obtained, 10 of the 122 seismic events were identified as natural, and 96 were determined to be artificial, resulting in a general success rate of 86.89%. However, classification results for 16 seismic events were inconclusive with the methods used. As a result, more detailed secondary analyses should be conducted to accurately determine the source types of micro-seismic events, and the seismic catalogs should be updated accordingly.

1. Introduction

Cyprus is an island country located in the Mediterranean, which is not only rich in historical and cultural heritage but also draws significant attention in terms of tourism. Particularly due to the impact of tourism, there is an increase in construction and, consequently, a demand for industrial raw materials driven by the expansion of the intra-island road transportation infrastructure. The provision of material needs from its own internal resources is facilitated by certain quarry operations located on the island. These quarry operations, where materials are obtained using explosive and combustible substances, exhibit micro-scale ground vibrations during their activities. These vibrations are recorded by seismic stations and documented in earthquake catalogs.

The tectonic control of the region is mainly provided by the Cyprus Arc, which passes through the southern part of the island in general; it is also supported by the Kyrenia Range (Girne-

Cite as: E. Yavuz (2024). Characterization of Micro-seismic Activity in Northern Cyprus Using Complexity and Corner Frequency Methods, *Sakarya University Journal of Science,* 28(4), 884-898. https://doi.org/10.16984/saufenbilder.1351756

This is an open access paper distributed under the terms and conditions of the Creative Commons Attribution-NonCommercial 4.0 International License.

Beşparmak Ridge) to the north and partially oblique-slip faults developing to the east and west. As a result, it is observed that not only micro-scale artificial vibrations but also tectonic events of similar scales are recorded in the region. The low energy content of these micro-scale activities, the limited number of recording stations, their small size resulting in noisy recordings, and the fact that they are not subjected to detailed analysis by the seismology center responsible for cataloging, sometimes lead to their omission from earthquake catalogs, or they are inaccurately categorized under the wrong source type. Erroneous micro-seismic catalogs mislead researchers and can even result in secondary studies, causing both time and workload burdens.

Due to these reasons, various methods have been employed to distinguish natural and artificial vibrations from the past to the present. The initial studies on this subject were conducted mainly in the United States [1-4]. While simple methods like amplitude ratio and complexity provide some direction, results obtained in the frequency domain also offer reliable information about source type identification based on signal characteristics. One of the first examples of the complexity method was conducted by [5] to differentiate underwater explosions. The same method was applied to short-period seismograms by [6]. In Türkiye, complexity analysis has been applied through earthquake stations located in various cities, such as Istanbul, Eastern Black Sea Region, Sakarya, Yalova-Bursa Gaziantep-Kahramanmaras and Edirne [7-12].

In the US, discrimination analysis using high-frequency waves was conducted by [13], natural and artificial vibrations around the Vertes Mountains in Hungary were studied by [14], and seismic events of two different types in various regions of Egypt were analyzed using the complexity method by [15, 16]. Furthermore, in recent years, corner frequency methods are being employed worldwide to characterize natural and artificial vibrations. [17] determined source type using corner frequency-magnitude relationship on 2430 events at the Israel-Lebanon border. [18] discriminated earthquakes from controlled explosions near Mount St. Helens using corner frequencies of *P* and *S* waves. [19] applied a similar method in the western US. [20] tested tree-based machine learning methods using the complexity approach. [21] combined the corner frequency and magnitude relationship with deep learning for source type identification. In seismic active regions of Egypt, [22-24] applied discrimination analysis based on the spectra of *P* and *S* waves.

In the study, complexity and corner frequency methods were employed using vertical components of events recorded at the seismic station LFK operated by the Boğaziçi University Kandilli Observatory and Earthquake Research Institute Regional Earthquake-Tsunami Monitoring Center (KOERI-RETMC) with local magnitudes of M≤2.7 that occurred in the northern part of Cyprus. In order to classify the obtained parameters, Linear Discriminant Function (LDF) and Quadratic Discriminant Function (QDF) were employed to determine the source types of these seismic events. The obtained results, along with statistical approaches, can be used to update the existing earthquake catalogs and will serve as a key in classifying future seismic events. Consequently, aiming for the emergence of more reliable earthquake catalogs, this will reduce the need for secondary analyses, leading to a decrease in time loss and workload.

2. Geological and Tectonic Structure

Northern Cyprus consists of three main geological belts from south to north, which are respectively Troodos Ophiolite, Troodos Surrounding Sedimentary Sequence, and the Besparmak Region [25]. While Quaternary alluvial forms shape the northern coast of the region, as one moves southward from the coast, the dominance of Oligocene sedimentary rock units belonging to the Degirmenlik Group, including sandstones, conglomerates, and mudstones, can be observed. Within this group, Eocene-aged carbonate deposits running parallel to the east/northeast-west Girne-Beşparmak Ridge (Degirmenlik Fault), Mesozoic-aged dolomitized carbonate rocks forming the main elevation of the Beşparmak Mountains, known as the Tripa Group, and Late Cretaceous-Eocene-aged mudstones, limestone, and volcanics

forming the Lapta Group are present [26-29] (Figure 1).
To fulfill the industrial raw material needs of the region, some open quarry operations in certain areas of these formations carry out their activities through controlled explosions. Thus, micro-scale ground vibrations are also documented in seismic centers' earthquake catalogs.

The island is tectonically controlled by the Cyprus Arc, extend to the south, an area where the African and Anatolian Plates collide at a rate of 10 mm/year, generating both destructive and tsunami-generating earthquakes in the past [30-33]. The northern part of the island, which is the study area, is dominated by the Degirmenlik Fault (Girne-Beşparmak Ridge), extending parallel to the Beşparmak Mountains and producing earthquakes on a smaller scale [29, 34] (Figure 1).

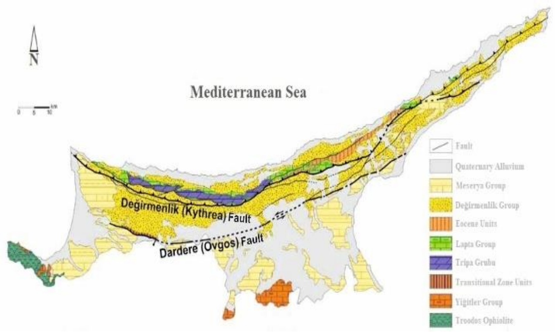
N
Mediterranean Sea
0 5 10 km
Değirmenlik (Kythrea) Fault
Dardere (Ovgos) Fault
Fault
Quaternary Alluvium
Meserya Group
Değirmenlik Group
Eocene Units
Lapta Group
Tripa Grubu
Transitional Zone Units
Yiğitler Group
Troodos Ophiolite

Figure 1. Simplified geological map of Northern Cyprus (Adapted from [29])

In the study area, micro-scale natural and anthropogenic-induced vibrations are recorded and cataloged by seismology centers. However, due to their low energy content, difficulties can arise in determining both the epicenter and source types of these vibrations. As a result, incorrect identifications in catalogs become prominent, leading to erroneous outcomes in new endeavors such as seismology, seismotectonics, hazard analysis, and more. This can either result in misleading conclusions or necessitate secondary analyses, leading to time loss and added workload for researchers.

3. Data Set

In the study, a GURALP-3ESP sensor-equipped seismic station with the station code LFK, operated by KOERI-RETMC, located at coordinates 35.2832°N - 33.5335°E in the vicinity of Nicosia, at an elevation of 690 meters above sea level, and configured to sample at a rate of 100 samples per second was used. Vertical component seismograms of 122 seismic events with magnitudes ranging from $0.9 \leq Ml \leq 2.7$, characterized by high signal quality, absence of digitization errors, and reliable phase readings, were employed for the analysis of micro-seismic activity (Figure 2).

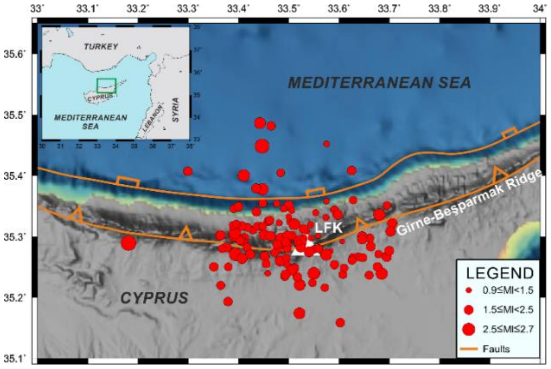
33°
33.1°
33.2°
33.3°
33.4°
33.5°
33.6°
33.7°
33.8°
33.9°
34°
35.6°
35.5°
35.4°
35.3°
35.2°
35.1°
TURKEY
CYPRUS
MEDITERRANEAN SEA
LEBANON
SYRIA
MEDITERRANEAN SEA
LFK
Girne-Beşparmak Ridge
CYPRUS
LEGEND
0.9≤Ml<1.5
1.5≤Ml<2.5
2.5≤Ml≤2.7
Faults

Figure 2. Tectonic structure of the study area and epicentral distribution of the seismic events. Faults are adapted from [34]

The events exhibit distances to the station ranging from 1 to 30 km, surrounding the station LFK from various directions. The epicenters for the 122 seismic events obtained by KOERI-RETMC are generally determined using 3 to 18 seismic stations and 4 to 19 phase picks (*P*, *S*), with azimuthal gap values varying between 70 and 349 degrees (Figure 3, Appendix A). Consequently, it has been determined that the low number of stations and phase readings, as well as the partially substantial azimuthal gap, play a role in locating micro-seismic activity. In the region where quarry blasts are frequent, records of a thorough analysis can be observed only for the station LFK, and a reliable assessment has been made with only one station.

Therefore, taking into consideration the potential location and depth errors that could arise due to the low number of existing stations on the island and the low energy content of micro-seismic events, along with the possibility of unauthorized explosions, seismic records were examined over a 4-year period from January 2018 to December 2021 (continuing in current open-pit quarry operations).

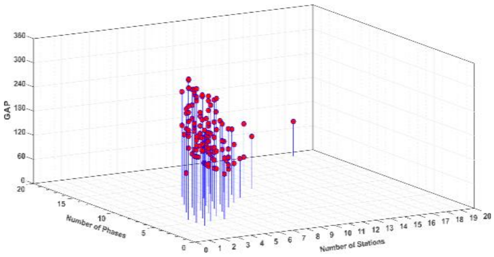

Figure 3. Azimuthal gap (GAP) along with the numbers of stations and phases used in the epicentral solution of the 122 events

4. Method

In the study, a total of 122 events with magnitudes ranging from 0.9≤Ml≤2.7, recorded at the seismic station LFK operated by KOERI-RETMC, were analyzed using complexity and corner frequency methods. For both methods, Linear Discriminant Function (LDF) and Quadratic Discriminant Function (QDF) were employed to classify the results.

In order to apply LDF and QDF analyses, the source types of the seismic events need to be initially defined. KOERI-RETMC determines the source type without resorting to technical analyses, solely based on observation and field knowledge. Therefore, the initial categorization was done on a case-by-case basis. As a result, preliminary information about source types was obtained through observational analyses such as amplitude of *P* and *S* waves, first motion direction of *P* waves, observation of *R*g phase, and decay rate of coda waves, based on the vertical component seismograms recorded at the station LFK (Figure 4).

Theoretically, the amplitudes of S-waves for quarry blast signals are significantly lower compared to *P*-wave amplitudes in vertical component seismograms, whereas for earthquakes, it is vice versa. The *P*-wave first motion direction generally tends to be positive for quarry blasts, while it is varies for earthquakes. In quarry blasts signals with a close epicentral distance, the emergence of the *R*g wave phase is generally observed. The attenuation of tectonic events is characterized by a logarithmic decay and extended duration, whereas for explosions, it is vice versa [9, 10, 35, 36].

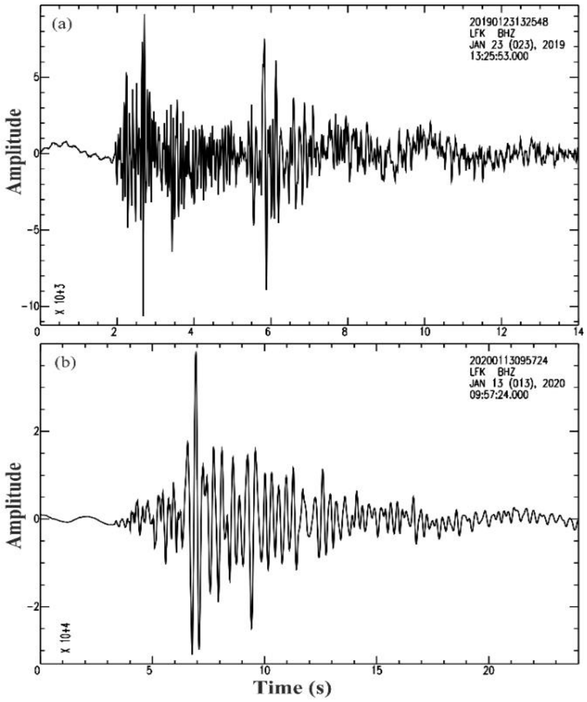

Figure 4. a) Vertical component seismograms of the earthquake on 23.01.2019 at 13:25:48.48 (Ml=1.6) and b) quarry blast on 13.01.2020 at 09:57:24.40 (Ml=1.8) recorded at the station LFK

In seismology, the complexity method, which is user-friendly and quick, is commonly employed to determine the source types of natural and anthropogenic vibrations. Within this method, two distinct parameters, namely complexity and spectral ratio, are computed and their relationships are compared graphically [5, 6]. In this approach, vertical component seismograms are divided into two separate time windows (t_o-t_1, t_1-t_2), and their powers ($s^2(t)$) are calculated to determine the complexity (C) parameter (Equation 1). Subsequently, by considering the two windows holistically, a two-stage band-pass filter (h_1-h_2, l_1-l_2; high and low corner frequencies) is applied to calculate the spectral ratio-a(f) parameter, denoted as *Sr* (Equation 2).

$$C = \int_{t_1}^{t_2} s^2(t)dt / \int_{t_0}^{t_1} s^2(t)dt \qquad (1)$$

$$Sr = \int_{h_1}^{h_2} a(f)df / \int_{l_1}^{l_2} a(f)df \qquad (2)$$

The low and high-frequency values are directly related to the frequency content of the signals and have been optimally determined for this study as 5-10 Hz and 1-5 Hz, respectively.

It is known that earthquakes and quarry blasts exhibit differences in their spectra due to their source mechanisms. In explosions, signals dominated primarily by *P*-waves are obtained, as explosions are predominantly characterized by a single-point source. In contrast, even though earthquakes may have lower energy, they occur through a linear source mechanism, resulting in the generation of higher-amplitude *S*-waves [36]. Spectra of earthquakes recorded in close proximity show energy distributed over a broader frequency range and damping at higher corner frequencies. In contrast, this behavior is reversed in explosions [10, 17, 37, 38].

Theoretically, there is a direct relationship between the corner frequency and the magnitude of a seismic event [39, 40]. Thus, corner frequency values (*fc*) for each event are calculated from vertical component seismograms due to the whole waveform (*P* to final), while local magnitudes (Ml) are directly obtained from KOERI-RETMC catalogs.

Both complexity and corner frequency method parameters are represented on a graph. To determine the source type, a third group alongside the parameters corresponding to the horizontal and vertical axes is introduced, and Linear and Quadratic Discriminant Functions (LDF and QDF) are employed. These statistical approaches are based on classification techniques using the principle of calculating the smallest error for data from different groups generated from different normal distributions [41-44].

For LDF, a single covariance matrix is determined for all groups, whereas for QDF, a separate covariance matrix is provided for each group [45]. The formulas for LDF and QDF are shown in Equation 3 and Equation 4.

$$F_{LDF}=K+L(1)*x+L(2)*y \tag{3}$$

$$F_{QDF}=K1+[x \quad y]*L1+\sum\{([x \quad y]*Q1)*[x \quad y]\} \tag{4}$$

Here, the parameter K represents the constant value of the boundary equation, while the parameters L and Q respectively denote the linear and quadratic coefficients of the same equation system.

5. Results

In this study, vertical component seismograms of 122 events recorded at the seismic station LFK, operated by KOERI-RETMC, and ranging in magnitude from 0.9≤Ml≤2.7, were subjected to complexity and corner frequency methods for analysis. Considering the errors in determining source types in KOERI-RETMC catalogs, the event types were initially determined through visual analysis. Of the 122 events in the KOERI-RETMC catalogs, 87 were identified as artificial and 35 as natural. However, visual examination in this study revealed that these numbers were actually 109 and 13, respectively (Table 1, Appendix A). Accordingly, based on the aforementioned initial categorization, classification of seismic events using discriminant functions was performed.

In general, it is observed that artificial events are more successfully discriminated compared to natural ones (Table 1). The signal characteristics of quarry blasts are known to be more consistent depending on the distance to the epicenter, while earthquakes exhibit a more complex distribution due to their different mechanisms. Therefore, artificial events are more effectively distinguished. While earthquakes were classified with full success using the corner frequency method, a discrimination rate of approximately 95.41% for explosions in the complexity method and 85.21% for corner frequency method was observed. However, when examined based on the methods, the corner frequency method achieved a success rate of up to 87%, while the complexity analysis reached a success rate of up to 91% (Table 1). The QDF applied to the complexity method yielded a slightly higher success rate of 90.98% compared to the LDF result of 90.16% (Table 1, Figure 5). Both discriminant functions achieved a source type classification success rate of 86.89% in the corner frequency method (Table 1, Figure 6). Although similar results were obtained between the discriminant functions, it was observed that QDF provided slightly better results than LDF. Furthermore, as a second-degree function, QDF demonstrated more reliable discriminant analysis compared to LDF, which is a first-degree function. The parameters of the functions are shown in Table 2.

Table 1. Analysis results based on method and statistical approach. LDF: Linear Discriminant Function, QDF: Quadratic Discriminant Function, E: Earthquake, B: Blast, M-E: Misclassified Earthquake, M-B: Misclassified Blast

Method	Statistical Approach	Numbers				Success Rate (%)		
		E	B	M-E	M-B	E	B	Overall
KOERI-RETMC		35	87	-	-	-	-	-
Initial Categorization		13	109	-	-	-	-	-
Complexity	LDF	6	104	7	5	46.15	95.41	90.16
	QDF	7	104	6	5	54.85	95.41	90.98
Corner Frequency	LDF	13	93	-	11	100.00	85.21	86.89
	QDF	13	93	-	11	100.00	85.21	86.89
Final Result		10	96	16		-	-	86.89

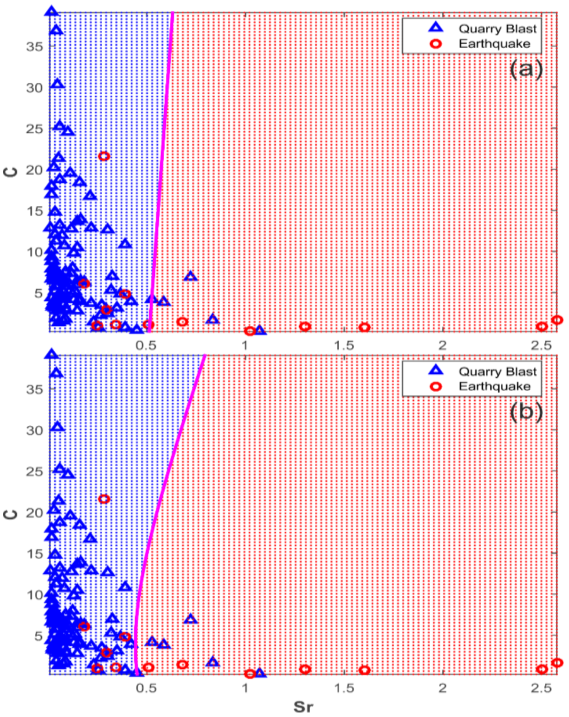

Figure 5. a) LDF b) QDF graphs for the Complexity method

To determine the source types of seismic events, all methods and statistical analyses were jointly evaluated, resulting in the identification of 10 events as earthquakes and 96 events as quarry blasts out of the analyzed 122 ground shaking events. Additionally, 16 events exhibited different outcomes when the aforementioned methods and discriminant functions were employed, hence they were classified as unidentified events after this study. As a result, a general success rate of 86.89% was achieved for the classification of the source types of 122 events (Table 1, Figure 7, Appendix A).

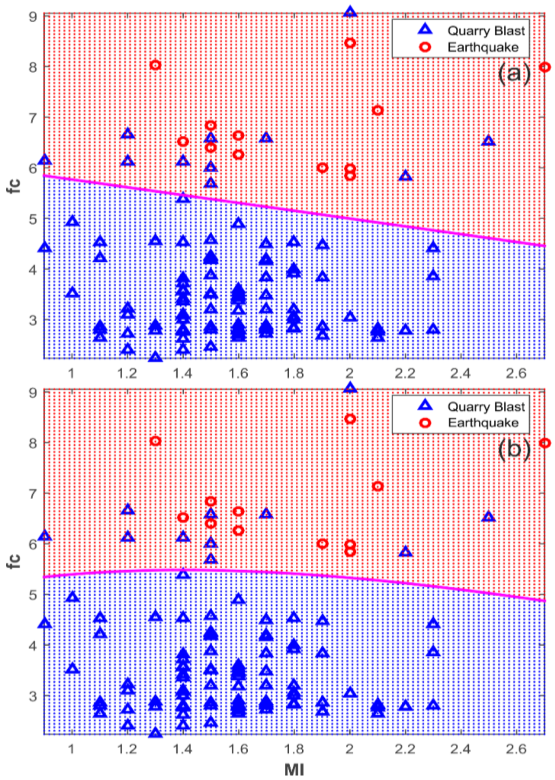

Figure 6. a) LDF b) QDF graphs for the Corner Frequency method

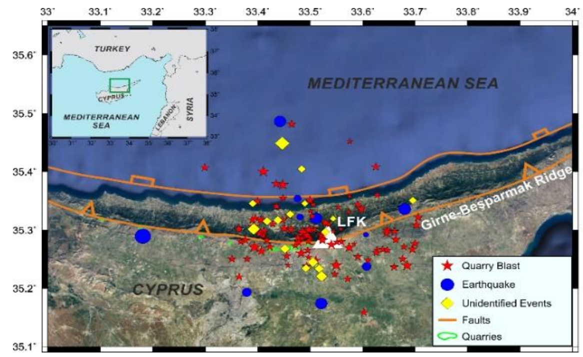
33°
33.1°
33.2°
33.3°
33.4°
33.5°
33.6°
33.7°
33.8°
33.9°
34°
35.6°
35.5°
35.4°
35.3°
35.2°
35.1°
TURKEY
CYPRUS
MEDITERRANEAN SEA
LEBANON
SYRIA
MEDITERRANEAN SEA
LFK
Girne-Beşparmak Ridge
CYPRUS
Quarry Blast
Earthquake
Unidentified Events
Faults
Quarries

Figure 7. Distribution of source types obtained after the analyses. Faults from Seyitoğlu et al., 2022, and locations of quarries obtained from Google Earth Pro

Table 2. The discrimination functions of station LFK

Complexity	$F_{LDF}=4.0098+[-7.8357 \quad 0.0239]*\begin{bmatrix}Sr\\C\end{bmatrix}$
	$F_{QDF}=(1.1363)+[5.1763 \quad 0.0203]*\begin{bmatrix}Sr\\C\end{bmatrix}+[Sr \quad C]*\begin{bmatrix}-17.0587 & -0.0779\\-0.0779 & -0.0063\end{bmatrix}*\begin{bmatrix}Sr\\C\end{bmatrix}$
Corner Frequency	$F_{LDF}=15.5270+[-1.8324 \quad -2.3743]*\begin{bmatrix}Ml\\fc\end{bmatrix}$
	$F_{QDF}=(19.3113)+[8.0652 \quad -6.0939]*\begin{bmatrix}Ml\\fc\end{bmatrix}+[Sr \quad C]*\begin{bmatrix}-1.5012 & -0.3523\\-0.3523 & -0.3711\end{bmatrix}*\begin{bmatrix}Ml\\fc\end{bmatrix}$

5. Conclusion and Discussion

In this study, source type determination analysis of 122 seismic events recorded in Northern Cyprus and cataloged by KOERI-RETMC was conducted using complexity and corner frequency methods, through Linear and Quadratic Discriminant Functions. The results reveal that the complexity method yields more successful outcomes compared to the corner frequency analysis, and similarly, the Quadratic Discriminant Function outperforms the Linear Discriminant Function. According to the obtained results, the source types of 10 earthquakes and 96 quarry blasts were reliably identified, while the source types of 16 events could not be determined. As a result, the overall success rate was calculated as 86.89%.

Seismic centers employ various seismic stations, algorithms, and crustal structures, and in user-based studies, different phase picks are made. Therefore, differences in the determination of location, magnitude, depth, and particularly source type are observed for seismic events, especially at the micro-scale. KOERI-RETMC identifies the source type solely based on proximity to quarry blast areas and visual inspection, without resorting to technical analysis.

Erroneous source type identification in micro-seismic activity can be rectified by secondary analyses, resulting in more reliable catalog descriptions. Updating past catalogs and comprehensively examining future seismic events can minimize error margins, ensuring the presentation of the most reliable results. This approach can facilitate the creation of more reliable earthquake catalogs for studies such as seismology, seismotectonics, seismicity, and earthquake hazard analysis, while eliminating the need for researchers to engage in time-consuming secondary analyses.

Due to the limited number of stations across the island and the considerable distance from stations in Türkiye, the error rates in location solutions of seismic events increase, leading to challenges in determining the source types. Therefore, increasing the number of stations throughout the island, and even deploying seafloor seismometers in the surrounding waters, is recommended not only for identifying artificial events but also for revealing the region's active tectonic activity more clearly

Article Information Form

Acknowledgments

The seismograms used in the study were obtained from the database of the Boğaziçi University Kandilli Observatory and Earthquake Research Institute Regional Earthquake-Tsunami Monitoring Center (KOERI-RETMC).

Funding

The author (s) has no received any financial support for the research, authorship or publication of this study.

The Declaration of Conflict of Interest/ Common Interest

No conflict of interest or common interest has been declared by the authors.

The Declaration of Ethics Committee Approval

This study does not require ethics committee permission or any special permission.

The Declaration of Research and Publication Ethics

The authors of the paper declare that they comply with the scientific, ethical and quotation rules of SAUJS in all processes of the paper and that they do not make any falsification on the data collected. In addition, they declare that Sakarya University Journal of Science and its editorial board have no responsibility for any ethical violations that may be encountered, and that this study has not been evaluated in any academic publication environment other than Sakarya University Journal of Science.

Copyright Statement

Authors own the copyright of their work published in the journal and their work is published under the CC BY-NC 4.0 license.

References

[1] E. J. Kelly, "A Study of Two-short-period Discriminants," MIT Lincoln Laboratory, pp. 60, 1968.

[2] R. Blandford, "Discrimination between earthquakes and underground explosions," Annual Review of Earth and Planetary Science, vol. 5, no. 1, pp. 111-122, 1977.

[3] T. J. Bennett J. R. Murphy, "Analysis of seismic discrimination capabilities using regional data from western United States events," Bulletin of the Seismological Society of America, vol. 76, no. 4, pp. 1069-1086, 1986.

[4] S. R. Taylor, N. W. Sherman, M. D. Denny, "Spectral discrimination between NTS explosions and western United States earthquakes at regional distances," Bulletin of the Seismological Society of America, vol. 78, no. 4, pp. 1563-1579, 1988.

[5] Y. Gitterman, A. Shapira, "Spectral discrimination of underwater explosions," Israel Journal of Earth Sciences, vol. 42, pp. 37-44, 1993.

[6] N. Arai, Y. Yosida, "Discrimination by short-period seismograms," International Institute of Seismology and Earthquake Engineering, Building Research Institute (IISEE). Lecture Note, Global Course, Tsukuba, Japan, p. 10, 2004.

[7] G. Horasan, A. B. Güney, A. Küsmezer, F. Bekler, Z. Öğütçü, N. Musaoğlu, "Contamination of seismicity catalogs by quarry blasts: An example from Istanbul and its vicinity, northwestern Turkey," Journal of Asian Earth Sciences, vol. 34, pp. 90-99, 2009.

[8] Ş. Yılmaz, Y. Bayrak, H. Çınar, "Discrimination of earthquakes and quarry blasts in the eastern Black Sea region of Turkey," Journal of Seismology, vol. 17, pp. 721-734, 2013.

[9] E. Budakoğlu, G. Horasan, "Classification of seismic events using linear discriminant function (LDF) in the Sakarya region, Turkey," Acta Geophysica, vol. 66, no. 1, pp. 895-906, 2018.

[10] E. Yavuz, F. Sertçelik, H. Livaoğlu, H. Woith, B. G. Lühr, "Discrimination of quarry blasts from tectonic events in the Armutlu Peninsula, Turkey," Journal of Seismology, vol. 23, pp. 59-76, 2019.

[11] E. Yavuz, H. Livaoğlu, T. S. Irmak, F. Sertçelik, "Gaziantep-Kahramanmaraş Bölgesinde Meydana Gelen Deprem ve Taş Ocağı Patlatmalarının Zaman ve Frekans Ortamı Yöntemleri ile Sınıflandırılması," Bitlis Eren Üniversitesi Fen Bilimleri Dergisi, vol. 8, no. 2, pp. 642-651, 2019.

[12] A. Tan, G. Horasan, D. Kalafat, A. Gülbağ, "Discrimination of earthquakes and quarries in the Edirne district (Turkey) and its vicinity by using a linear discriminate function method and artificial neural networks," Acta Geophysica, vol. 69, no. 1, pp. 17-27, 2021.

[13] W. Y. Kim, D. W. Simpson, P. G. Richards, "Discrimination of earthquakes and explosions in the eastern United States using regional high-frequency data"

Geophysical Research Letters, vol. 20, no. 14, pp. 1507-1510, 1993.

[14] M. Kiszely, B. Süle, P. Mónus, I. Bondár, “Discrimination between local earthquakes and quarry blasts in the Vértes Mountains, Hungary,” Acta Geodaetica et Geophysica, vol. 56, no. 3, pp. 523-537, 2021.

[15] A. Badawy, M. Gamal, W. Farid, M. S. Soliman, “Decontamination of earthquake catalog from quarry blast events in northern Egypt,” Journal of Seismology, vol. 23, no. 6, pp. 1357-1372, 2019.

[16] I. M. Korrat, A. Lethy, M. N. ElGabry, H. M. Hussein, A. S. Othman, “Discrimination Between Small Earthquakes and Quarry Blasts in Egypt Using Spectral Source Characteristics,” Pure and Applied Geophysics, vol. 179, no. 2, pp. 599-618, 2022.

[17] G. Ataeva, Y. Gitterma, A. Shapira, “The ratio between corner frequencies of source spectra of P-and S-waves—a new discriminant between earthquakes and quarry blasts,” Journal of Seismology, vol. 21, pp. 209-220, 2017.

[18] R. Wang, B. Schmandt, E. Kiser, “Seismic discrimination of controlled explosions and earthquakes near Mount St. Helens using P/S ratios” Journal of Geophysical Research: Solid Earth, vol. 125, no. 10, e2020JB020338, 2020.

[19] R. Wang, B. Schmand, M. Holt, K. Koper, “Advancing Local Distance Discrimination of Explosions and Earthquakes With Joint P/S and ML-MC Classification,” Geophysical Research Letters, vol. 48, no. 23, e2021GL095721, 2021.

[20] E. Yavuz, M. C. Iban, E. Arpaz, “Identifying the source types of the seismic events using discriminant functions and tree-based machine learning algorithms at Soma Region, Turkey,” Environmental Earth Sciences, vol. 82, no. 11, pp. 1-15, 2023.

[21] Q. Kong, R. Wang, W. R. Walter, M. Pyle, K. Koper, B. Schmandt, “Combining Deep Learning With Physics Based Features in Explosion-Earthquake Discrimination,” Geophysical Research Letters, vol. 49, no. 13, e2022GL098645, 2022.

[22] A. Lethy, A. Othman, M. ElGabry, H. Hussein, G. El-Qady, “Discrimination between Small Earthquakes and Local Quarry Blasts Using Committee Machine”, ResearchSquare, 2021.

[23] H. Saadalla, H. E. Abdelhafiez, T. Hayashida, “Discrimination between earthquakes and quarry blasts in the Aswan region, southern Egypt, using P-wave source spectra,” Journal of Seismology, vol. 27, no. 2, pp. 279-289, 2023.

[24] I. M. Korrat, M. N. Elgabry, A. Lethy, H. M. Hussein, E. Yavuz, A. S. Othman, “Discrimination of quarry blasts from earthquakes in Northern and Central Egypt using linear and quadratic discriminant functions,” Journal of Seismology, vol. 27, no. 4, pp. 609-626, 2023.

[25] CGSD (Cyprus Geological Survey Department), 1995. Geological Map of Cyprus, Scale 1/250.000, Nicosia, Cyprus.

[26] F. R. S. Henson, R. V. Browne, J. McGinty, “A synopsis of the stratigraphy and geological history of Cyprus,” The Quarterly Journal of the Geological Society of London, vol. 105, pp. 1-41, 1949.

[27] C. Ducloz, “Notes on the geology of the Kyrenia Range,” Cyprus Geological survey Dept., Annual Report for 1963, pp. 57-67, 1964.

[28] İ. Ketin, “A comparison between the tectonic uits of Cyprus and the Southern Taurus - Amanos Mountains” METU Journal of Pure and Applied Sciences, vol. 21/1-3, pp. 169-182, 1988.

[29] H. Y. Hakyemez, “Kuzey Kıbrıs’ın Temel Jeolojik Özellikleri,” TPJD Bülteni, vol. 26, no. 2, pp. 7-46, 2014.

[30] S. McClusky, R. Reilinger, S. Mahmoud, D. Ben Sari, A. Tealeb, “GPS constraints on Africa (Nubia) and Arabia plate motions,” Geophysical Journal Int., vol. 155, no.1, pp. 126-138, 2003.

[31] R. Reilinger, S. McClusky, P. Vernant, S. Lawrence, S. Ergintav, R. Cakmak, ... G. Karam, “GPS constraints on continental deformation in the Africa-Arabia-Eurasia continental collision zone and implications for the dynamics of plate interactions,” Journal of Geophysical Research: Solid Earth, vol. 111(B5), 2006.

[32] S. Yolsal, T. Taymaz, A. C. Yalçiner, “Understanding tsunamis, potential source regions and tsunami-prone mechanisms in the Eastern Mediterranean,” Geological Society, London, Special Publications, vol. 29, no. 1, pp. 201-230, 2007.

[33] S. Yolsal-Çevikbilen, T. Taymaz, “Earthquake source parameters along the Hellenic subduction zone and numerical simulations of historical tsunamis in the Eastern Mediterranean,” Tectonophysics, vol. 536, pp. 61-100, 2012.

[34] G. Seyitoğlu, E. Tunçel, B. Kaypak, E. Korhan, E. Gökkaya, “The Anatolian Diagonal: a broad left-lateral shear zone between the North Anatolian Fault Zone and the Aegean/Cyprus arcs,” Türkiye Jeoloji Bülteni, vol. 65, no. 2, pp. 93-116, 2022.

[35] M. A. Hedlin, J. B. Minster, J. A. Orcutt, “The time-frequency characteristics of quarry blasts and calibration explosions recorded in Kazakhstan, USSR,” Geophysical Journal International, vol. 99, no. 1, 109-121, 1989.

[36] P. Bormann, “New manual of seismological observatory practice,” 2002.

[37] P. M. Shearer, B. P. Allmann, “Spectral studies of shallow earthquakes and explosions in Southern California,” Proceedings of the 29th Monitoring Research Review: Ground-Based Nuclear Explosion Monitoring Technologies, pp. 656-662, 2007.

[38] B. P. Allmann, P. M. Shearer, E. Hauksson, “Spectral discrimination between quarry blasts and earthquakes in southern California,” Bulletin of the Seismological Society of America, vol. 98, no. 4, pp. 2073-2079, 2008.

[39] T. C. Hanks, D. M. Boore, “Moment-magnitude relations in theory and practice,” Journal of Geophysical Research: Solid Earth, vol. 89(B7), pp. 6229-6235, 1984.

[40] T. S. Irmak, E. Yavuz, H. Livaoğlu, E. Şentürk, E. Y. Sahin, “Source parameters for small-moderate earthquakes in Marmara Region (Turkey),” Geosciences Journal, vol. 24, pp. 541-555, 2020.

[41] R. A. Fisher, “The use of multiple measurements in taxonomic problems” Annals of Eugenics, vol.7, no. 2, pp. 179-188, 1936.

[42] G. A. F. Seber, “Multivariate Observations,” Hoboken, John Wiley & Sons Inc., 1984.

[43] W. J. Krzanowski, “Principles of multivariate analysis: a user’s perspective,” Clarendon, 1988.

[44] V. Franc, V. Hlavác, “Statistical pattern recognition toolbox for Matlab,” Prague, Czech: Center for Machine Perception, Czech Technical University, 2004.

[45] H. S. Kuyuk, E. Yildirim, E. Dogan, G. Horasan, “Clustering seismic activities using linear and nonlinear discriminant analysis,” Journal of Earth Science, vol. 25, pp. 140-145, 2014.

Appendix A. The information of 122 seismic events and the results of the analysis. NoS: number of stations,
type, KOERI: Bogazici University Kandilli Observatory and Earthquake Research Institute Regional Earthqu
initial categorization, fc/CF: corner frequency, C: complexity, SR: spectral ratio, LDF: Linear Discriminant Fu
Function, EQ: earthquake, QB: quarry blast, UI: unidentified event.

Date	Origin Time (GMT)	Latitude (o)	Longitude (o)	NoS	NoP	GAP	ML	ST (KOERI)	ST (IC)	fc	C	SR	Com
													LD
03.01.2018	09:41:02.45	35.3228	33.4805	4	6	244	1.2	QB	QB	6.116	6.831	0.719	E
03.01.2018	10:42:48.37	35.3018	33.3923	5	8	190	2.2	QB	QB	5.829	1.435	0.229	Q
08.01.2018	09:53:34.29	35.3780	33.4477	6	8	177	2.1	QB	QB	2.761	24.481	0.099	Q
11.01.2018	09:26:06.74	35.2602	33.4828	7	8	122	1.9	QB	QB	2.866	4.106	0.132	Q
13.01.2018	13:43:12.65	35.3255	33.4597	6	10	113	1.6	QB	QB	2.782	2.747	0.095	Q
23.01.2018	09:56:10.96	35.2923	33.6063	4	6	301	0.9	EQ	QB	6.142	1.670	0.836	E
27.01.2018	10:14:39.81	35.2398	33.5498	5	6	214	2.2	QB	QB	2.785	18.695	0.060	Q
31.01.2018	10:26:38.11	35.2163	33.5715	6	9	146	1.4	EQ	QB	2.756	11.272	0.039	Q
06.02.2018	10:09:07.16	35.2210	33.5215	4	6	183	2.0	QB	QB	9.053	10.778	0.390	Q
09.02.2018	09:52:33.88	35.2763	33.5837	3	6	281	0.9	QB	QB	4.403	2.459	0.304	Q
16.02.2018	09:57:47.31	35.3443	33.5910	5	6	292	1.4	EQ	QB	3.407	7.945	0.123	Q
19.02.2018	14:23:22.51	35.2968	33.5287	5	9	254	1.5	QB	EQ	6.843	21.596	0.283	Q
20.02.2018	14:17:15.06	35.2713	33.6787	4	7	299	1.4	QB	QB	2.991	25.184	0.056	Q
26.02.2018	10:06:34.93	35.2908	33.4930	5	7	192	2.3	QB	QB	4.409	12.836	0.217	Q
08.03.2018	09:53:50.85	35.3015	33.5067	5	9	220	1.6	QB	QB	2.789	9.804	0.129	Q
10.03.2018	11:31:26.61	35.2797	33.5510	6	8	140	1.4	QB	QB	2.798	7.074	0.053	Q
15.03.2018	10:19:45.80	35.3513	33.4993	5	7	255	1.8	QB	QB	2.818	10.156	0.016	Q
20.03.2018	16:02:31.45	35.2803	33.5598	5	7	279	1.5	QB	QB	4.244	3.920	0.160	Q
27.03.2018	09:03:43.21	35.3542	33.4758	6	9	171	1.3	QB	EQ	8.037	1.395	0.682	E
28.03.2018	13:52:52.86	35.3603	33.6280	4	7	312	1.4	QB	QB	5.376	5.147	0.133	Q
29.03.2018	09:03:47.36	35.2967	33.4860	5	7	199	2.2	QB	QB	2.789	5.725	0.080	Q

06.04.2018	08:30:10.64	35.3458	33.3905	5	7	217	1.4	QB	QB	6.111	16.682	0.210	Q
06.04.2018	09:23:46.01	35.2678	33.4518	9	11	162	1.7	QB	QB	6.576	12.649	0.302	Q
13.04.2018	09:26:47.65	35.2508	33.3508	3	5	191	1.6	QB	QB	2.703	39.056	0.015	Q
19.04.2018	12:27:39.18	35.2348	33.4922	5	5	151	1.5	QB	EQ	6.406	6.026	0.184	Q
24.04.2018	09:55:51.55	35.3512	33.6955	3	6	326	1.4	QB	QB	3.071	0.336	1.071	E
25.04.2018	07:41:55.16	35.3017	33.5583	3	6	327	1.0	QB	QB	4.926	2.248	0.266	Q
30.04.2018	09:04:09.75	35.3030	33.4507	8	10	96	1.9	QB	QB	2.865	3.615	0.079	Q
30.04.2018	09:33:29.39	35.2848	33.5230	6	7	154	1.6	QB	QB	3.186	30.331	0.044	Q
30.04.2018	14:25:01.26	35.3363	33.5972	5	9	293	1.8	EQ	QB	2.845	8.068	0.029	Q
08.05.2018	08:09:51.62	35.3108	33.4287	5	7	200	1.4	QB	QB	3.567	10.515	0.148	Q
11.05.2018	15:03:48.71	35.3550	33.4483	3	5	302	1.5	QB	QB	4.167	6.100	0.105	Q
14.05.2018	09:03:39.46	35.3437	33.5060	4	8	256	1.2	QB	QB	3.22	3.466	0.269	Q
28.05.2018	09:08:44.65	35.3155	33.4175	6	8	100	1.5	QB	QB	6.003	3.651	0.219	Q
28.05.2018	09:14:05.84	35.2858	33.4847	5	5	112	1.2	QB	QB	3.108	6.284	0.180	Q
28.05.2018	09:17:09.07	35.3095	33.5353	6	7	176	1.3	QB	QB	2.885	21.310	0.052	Q
30.05.2018	07:53:53.46	35.3457	33.4898	3	5	311	1.3	QB	QB	4.553	3.754	0.587	E
30.05.2018	08:59:27.73	35.2712	33.3935	7	8	94	2.3	QB	QB	3.859	12.797	0.117	Q
30.05.2018	12:20:48.09	35.4818	33.4648	3	5	332	1.6	EQ	QB	3.434	13.666	0.146	Q
31.05.2018	12:57:38.67	35.4520	33.5753	3	6	349	1.1	EQ	QB	2.632	2.751	0.045	Q
10.12.2018	14:42:15.44	35.3178	33.4060	8	12	98	1.7	QB	QB	2.878	4.414	0.019	Q
13.12.2018	09:44:04.94	35.3220	33.7060	4	6	305	1.8	EQ	QB	3.991	2.751	0.149	Q
18.12.2018	10:01:10.25	35.2242	33.5470	9	13	191	1.4	QB	QB	3.094	2.781	0.048	Q
18.12.2018	12:02:22.44	35.2980	33.4115	9	14	85	1.7	QB	QB	2.81	7.105	0.042	Q
21.12.2018	10:00:29.64	35.2395	33.6848	4	7	225	2.1	EQ	QB	2.799	4.305	0.069	Q
24.12.2018	09:52:13.16	35.2917	33.5225	9	12	125	2.3	QB	QB	2.805	3.145	0.033	Q
26.12.2018	10:12:29.02	35.4487	33.4470	5	7	178	2.5	EQ	QB	6.526	4.800	0.367	Q
27.12.2018	11:23:41.12	35.2907	33.4102	4	6	183	1.4	QB	QB	2.799	1.512	0.076	Q

28.12.2018	09:47:27.72	35.2380	33.6078	5	8	234	1.5	EQ	QB	6.581	4.199	0.526	E
14.01.2019	10:40:10.76	35.2870	33.4993	3	6	206	1.3	QB	QB	2.774	36.845	0.042	Q
18.01.2019	09:48:35.06	35.2977	33.6610	7	9	207	1.6	EQ	QB	2.774	1.931	0.042	Q
21.01.2019	09:53:33.31	35.2982	33.5442	4	8	207	1.1	QB	QB	2.797	4.396	0.068	Q
23.01.2019	13:25:48.48	35.1935	33.3792	6	9	103	1.6	QB	EQ	6.642	0.890	2.504	E
24.01.2019	10:14:03.51	35.3012	33.4978	9	14	112	1.9	QB	QB	2.691	17.951	0.018	Q
25.01.2019	13:01:22.18	35.2507	33.3798	5	10	174	1.4	QB	QB	2.761	1.297	0.053	Q
31.01.2019	10:21:38.91	35.3410	33.4357	11	13	70	1.6	QB	QB	4.88	4.796	0.126	Q
04.02.2019	11:41:29.08	35.2895	33.1813	18	19	86	2.7	EQ	EQ	7.99	0.245	1.023	E
13.02.2019	10:43:59.88	35.3243	33.5037	5	8	243	1.4	QB	QB	2.625	7.036	0.033	Q
15.02.2019	08:45:41.67	35.2482	33.5108	5	6	161	1.7	QB	QB	2.808	3.232	0.022	Q
18.02.2019	09:56:13.77	35.3582	33.5747	5	7	291	1.1	QB	QB	4.528	3.101	0.350	Q
19.02.2019	10:10:42.48	35.3202	33.5438	3	6	346	1.2	QB	QB	6.667	7.031	0.326	Q
20.02.2019	08:51:46.79	35.2827	33.3763	4	8	97	1.7	QB	QB	4.16	4.202	0.158	Q
21.02.2019	08:14:46.47	35.3318	33.5740	5	7	162	1.2	QB	QB	2.406	5.820	0.039	Q
21.02.2019	11:52:25.42	35.2538	33.4973	7	8	123	1.3	QB	QB	2.234	6.436	0.027	Q
01.03.2019	10:41:37.98	35.2790	33.4780	8	9	97	1.6	QB	QB	2.792	12.838	0.008	Q
08.03.2019	08:56:47.97	35.3327	33.5000	4	8	245	1.1	QB	QB	2.857	7.450	0.024	Q
08.03.2019	12:53:31.77	35.3175	33.4383	4	7	227	1.5	QB	QB	5.691	6.422	0.146	Q
14.03.2019	09:54:59.35	35.2962	33.4055	7	8	104	1.5	QB	QB	4.578	18.383	0.162	Q
01.04.2019	09:00:56.14	35.2673	33.6948	6	9	216	1.8	QB	QB	3.053	3.481	0.021	Q
04.04.2019	08:50:51.65	35.3172	33.4480	6	9	155	1.4	QB	QB	3.812	7.573	0.091	Q
02.05.2019	08:49:00.89	35.2828	33.5233	5	6	118	1.8	QB	QB	3.2	6.761	0.054	Q
06.05.2019	09:29:38.13	35.2838	33.6630	5	8	209	1.7	EQ	QB	3.196	4.947	0.057	Q
07.05.2019	08:52:58.42	35.2540	33.5910	4	6	198	1.6	EQ	QB	3.473	7.933	0.034	Q
08.05.2019	12:16:15.58	35.2878	33.4763	4	6	169	1.6	QB	QB	2.825	8.890	0.022	Q
14.05.2019	09:38:19.31	35.2557	33.4552	7	10	132	1.5	QB	QB	4.189	7.314	0.117	Q

17.05.2019	08:30:36.83	35.2340	33.5170	7	8	194	1.6	QB	EQ	6.25	0.979	0.246	Q
23.05.2019	09:28:17.29	35.2807	33.4968	4	6	165	1.5	QB	QB	3.203	6.338	0.078	Q
24.05.2019	10:14:01.41	35.3272	33.4620	5	7	116	1.5	QB	EQ	6.834	4.859	0.390	Q
24.05.2019	10:19:07.71	35.2825	33.4173	5	7	122	1.5	QB	QB	2.855	5.205	0.035	Q
29.05.2019	11:34:58.92	35.3128	33.5293	7	10	106	1.7	QB	QB	2.846	9.309	0.019	Q
12.06.2019	09:34:05.95	35.2753	33.5405	11	12	129	1.9	QB	QB	3.835	13.907	0.168	Q
01.07.2019	09:09:56.39	35.3087	33.7025	4	7	305	1.8	QB	QB	3.91	3.462	0.079	Q
08.07.2019	09:21:29.38	35.2917	33.4937	6	9	138	1.6	QB	QB	2.641	6.476	0.041	Q
15.07.2019	09:38:38.47	35.2202	33.3647	9	10	97	1.5	QB	QB	4.236	0.390	0.449	Q
22.07.2019	08:54:11.49	35.3393	33.5537	4	5	287	1.2	QB	QB	2.714	10.747	0.081	Q
23.07.2019	09:14:57.84	35.3060	33.3922	7	11	87	2.1	QB	QB	2.649	5.680	0.042	Q
01.11.2019	09:57:24.80	35.2507	33.6763	5	7	223	1.6	EQ	QB	3.588	7.256	0.032	Q
10.12.2019	09:54:00.21	35.2940	33.4030	5	7	154	1.5	QB	QB	2.468	3.875	0.028	Q
18.12.2019	10:27:20.90	35.2653	33.4952	7	8	144	1.4	QB	QB	4.522	0.725	0.392	Q
23.12.2019	09:57:57.74	35.2400	33.4582	4	7	146	1.1	QB	QB	4.215	1.761	0.088	Q
13.01.2020	09:01:04.55	35.2738	33.4717	6	8	121	1.4	QB	QB	3.551	2.903	0.294	Q
13.01.2020	09:57:24.40	35.3005	33.6465	6	8	215	1.8	EQ	QB	3.007	7.831	0.019	Q
17.01.2020	09:37:22.01	35.2703	33.5745	4	7	208	2.0	EQ	QB	3.032	16.949	0.015	Q
03.02.2020	10:27:39.42	35.2367	33.6597	3	6	222	1.5	EQ	QB	3.502	6.837	0.042	Q
19.02.2020	10:07:34.54	35.2668	33.6382	4	5	217	1.5	QB	QB	3.514	6.729	0.075	Q
20.02.2020	10:28:00.09	35.1742	33.5213	3	4	236	2.0	EQ	EQ	5.836	1.100	0.511	Q
02.03.2020	09:57:26.78	35.2657	33.6472	4	7	218	1.5	EQ	QB	3.872	6.396	0.163	Q
06.03.2020	10:09:16.08	35.2955	33.6460	6	7	217	1.7	EQ	QB	3.477	6.949	0.044	Q
13.05.2020	09:01:21.64	35.3010	33.4637	6	8	152	1.8	QB	QB	4.537	5.320	0.320	Q
09.06.2020	09:24:17.34	35.3495	33.4000	6	9	155	1.7	QB	QB	2.715	13.195	0.059	Q
03.07.2020	09:18:43.83	35.2643	33.4067	6	8	270	1.9	QB	QB	4.48	3.900	0.422	Q
15.07.2020	09:09:06.12	35.3792	33.4353	3	5	180	1.7	EQ	QB	4.492	0.715	0.255	Q

16.07.2020	07:36:03.16	35.3180	33.3900	5	7	157	1.6	QB	QB	2.714	12.123	0.033	Q
24.07.2020	09:29:08.33	35.2447	33.5052	6	9	175	1.9	EQ	EQ	6.002	2.917	0.297	Q
12.08.2020	19:01:20.69	35.4863	33.4425	6	12	178	2.0	EQ	EQ	5.972	1.713	2.576	E
18.08.2020	08:59:38.13	35.2803	33.3675	5	9	133	1.4	QB	QB	2.408	20.246	0.028	Q
20.08.2020	01:38:24.70	35.3363	33.6803	11	13	153	2.1	EQ	EQ	7.136	0.786	1.600	E
04.09.2020	08:56:34.58	35.2488	33.6100	5	6	215	1.4	EQ	QB	3.571	2.992	0.059	Q
10.09.2020	09:14:00.90	35.4047	33.4838	3	6	266	1.4	EQ	EQ	6.525	1.076	0.342	Q
12.10.2020	08:07:49.53	35.1588	33.6025	3	6	177	1.6	EQ	QB	2.904	14.782	0.035	Q
14.10.2020	09:06:38.29	35.2378	33.4932	8	9	143	1.7	QB	QB	2.878	4.368	0.082	Q
01.12.2020	09:52:51.30	35.4087	33.6252	3	5	214	1.6	EQ	QB	3.539	5.159	0.074	Q
07.12.2020	10:17:01.83	35.2767	33.6998	4	7	223	1.7	EQ	QB	3.838	6.367	0.079	Q
26.01.2021	10:32:24.22	35.4007	33.4107	4	7	162	2.1	EQ	QB	2.821	19.583	0.109	Q
07.04.2021	09:35:24.63	35.3022	33.3643	6	10	162	1.8	QB	QB	2.813	8.842	0.017	Q
25.06.2021	09:32:57.48	35.3207	33.3958	3	6	243	1.4	QB	QB	3.352	4.278	0.051	Q
25.06.2021	09:39:55.31	35.2662	33.6273	5	8	159	1.4	EQ	QB	3.713	6.590	0.019	Q
09.07.2021	09:41:56.78	35.4075	33.2993	3	5	204	1.6	EQ	QB	3.374	2.999	0.086	Q
09.07.2021	09:49:58.75	35.2908	33.5200	3	5	163	1.0	QB	QB	3.519	3.258	0.036	Q
23.07.2021	23:39:17.44	35.3205	33.5113	7	11	136	2.0	EQ	EQ	8.474	0.819	1.300	E
20.09.2021	10:08:15.16	35.2710	33.4233	6	12	261	1.7	QB	QB	4.184	11.961	0.069	Q
02.11.2021	10:25:06.09	35.2613	33.6260	3	6	216	1.5	EQ	QB	2.804	5.904	0.148	Q